Multiobjective Optimization of Solar Flat Plate Collector Using Water Cycle Algorithm

Bao-Huy Truong[1], Thanh Tran Van[1], Thien Vo Minh[2], Tuan Duong Van[3], and Dieu Vo Ngoc[*4,5]

ARTICLE INFO

Article history:
Received: 2 December 2020
Revised: 23 February 2021
Accepted: 18 March 2021

Keywords:
Multiobjective optimization
Water Cycle Algorithm
Solar flat plate collector
Thermal efficiency
Total annual cost

ABSTRACT

This study proposes a Multiobjective Water Cycle Algorithm (MOWCA) for multiobjective optimization of flat plate solar collector (FPC). MOWCA was inspired by the process of water circulation. The proposed algorithm was implemented to simultaneously optimize the thermal efficiency and total annual cost (TAC) of FPC. The design parameters were mass flow rate, riser tube's outer diameter, tube number, and insulation thickness. The thermal efficiency and TAC obtained by MOWCA were 71.9541% and 78.2980 $/year for the best compromise solution, providing a balance between the two objectives. Moreover, the optimal results obtained by MOWCA were analyzed and compared to those from other algorithms. The comparative outcomes highlighted the effectiveness and robustness of the MOWCA to assist manufacturers in selecting appropriate design parameters for FPC.

1. INTRODUCTION

Global energy demand is dramatically increasing due to global population growth, technological development, and commercial and industrial activities [1]. Renewable energy is a sustainable and environmentally friendly source of energy, providing a perfect solution for limiting fossil fuel consumption and environmental issues from combustion processes for energy generation. Solar water heating system (SWH) is a potential application of renewable energy utilization. The solar thermal collector is a critical component of SWH in which a flat plate collector (FPC) is commonly used for low and medium thermal applications. Figure 1 depicts a diagram of a typical FPC. One of the most significant barriers and challenges for the development of SWH is the low thermal efficiency and high operational cost of the solar collector.

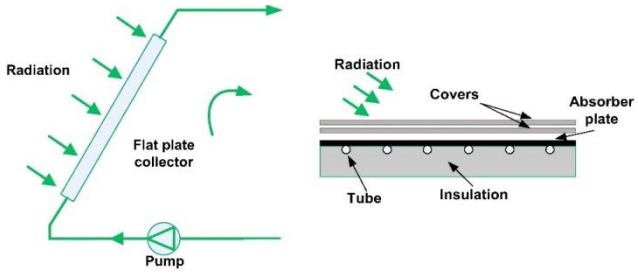

Fig. 1. Diagram of an FPC system [2].

Over the last decade, various studies proposed FPC optimization approaches with impressive results. Search Group Algorithm (SGA) [3] was suggested for a solar water heating (SWH) system using FPC that improved energetic efficiency by 4.904%. Farahat et al. [4] developed exergetic optimization by applying Sequential Quadratic Programming (SQP) to optimize FPC efficiency by minimizing exergy losses. Badr et al. [6] exploited a Genetic Algorithm's (GA) potential to optimize an active SWH with FPC under different environmental conditions and design parameters. Wenceslas [7] optimized a thermosyphon solar water heater using GA and optimized design parameters to fabricate an FPC with locally available materials. His system obtained higher efficiency with lower collector surface area. Khademi et al. [8] compared SQP versus GA to maximize FPC exergy performance. They found that GA optimization yielded higher accuracy but lower convergence speed than SQP.

In the literature, most studies were conducted to optimize the FPC efficiency without considering costs. FPC system should be concurrently optimized in terms of the thermo-economic viewpoints. There were only a few studies in multiobjective optimization of FPC. Hajabdollahi [2] analyzed Multiobjective Particle Swarm Optimization (MOPSO) to optimize cost and efficiency simultaneously. Hajabdollahi and Premnath [9] also applied MOPSO to minimize yearly cost and maximize

[1]*Institute of Engineering and Technology, Thu Dau Mot University, Binh Duong Province, Vietnam*
[2]*Faculty of Electrical, Electronics, and Telecommunication Engineering, Can Tho University of Engineering and Technology, Can Tho City, Vietnam*
[3]*Ho Chi Minh City Vocational College, Ho Chi Minh City, Vietnam*
[4]*Department of Power Systems, Ho Chi Minh City University of Technology (HCMUT), 268 Ly Thuong Kiet Street, District 10, Ho Chi Minh City, Vietnam*
[5]*Vietnam National University Ho Chi Minh, Linh Trung Ward, Thu Duc District Ho Chi Minh City, Vietnam.*
**Corresponding author:* Dieu Ngoc Vo; E-mail: vndieu@hcmut.edu.vn.

efficiency by analyzing effects from Al_2O_3 nanoparticles and various design parameters of FPC. In [10], an FPC system using CuO nanofluid was modeled and optimized using MOPSO. Hajabdollahi et al. [11] investigated effects on FPC systems from SiO_2, Al_2O_3, and CuO nanofluids in thermo-economic terms. Cost and efficiency were determined by using a Nondominated Sorting Genetic Algorithm II (NSGA-II). In general, most relevant studies have only applied conventional algorithms, named MOPSO and NSGA-II, without considering other methods. Besides, performance comparisons of multiobjective algorithms to deal with this issue have not been addressed.

This study proposed a first attempt of the Multiobjective Water Cycle Algorithm (MOWCA) for multiobjective optimization of FPC. The basic concept of MOWCA was based on the circulation of water in nature. The proposed method was applied to simultaneously optimize thermal efficiency and total annual cost (TAC) of FPC. Specification parameters of FPC, consisting of mass flow rate, riser tube's outer diameter, tube number, and insulation thickness, were considered as design variables. The MOWCA was implemented to offer non-dominated solutions and respective tradeoffs based on the two contradictory objectives: thermal efficiency and TAC. The obtained results were compared to other methods. Comparative outcomes emphasized the performance of MOWCA for the multiobjective optimization of FPC.

2. PROBLEM FORMULATION

2.1. Thermo-Economic Modeling of FPC

2.1.1. Thermal efficiency

The first objective function for thermal efficiency (η) of FPC is defined as [12]:

$$F_1 = \eta = \frac{Q_u}{A_c I_T} \tag{1}$$

where Q_u is useful heat gain, A_c is cover surface area, and I_T is total solar radiation intensity.

In steady-state conditions, the thermal energy balance of FPC is given as follows [13]:

$$Q_u = Q_{ab} - Q_{loss} \tag{2}$$

where Q_{ab} is the absorbed energy and Q_{loss} is the total heat loss.

Absorbed energy can be stated as:

$$Q_{ab} = A_p(\tau\alpha)I_T \tag{3}$$

where $(\tau\alpha)$ denote the effective transmittance-absorptance, and A_p is the absorber plate area.

Total heat loss is computed as:

$$Q_{loss} = A_c U_L (T_{pm} - T_a) \tag{4}$$

where T_{pm} denotes the absorber plate's mean temperature, T_a denotes the ambient temperature, and U_L is the overall heat loss coefficient.

The overall heat loss coefficient is expressed as follows:

$$U_L = U_t + U_e + U_b \tag{5}$$

The top loss coefficient can be given as follows [14]:

$$U_t = \left[\frac{N}{\frac{C}{T_{pm}}\left[\frac{T_{pm}-T_a}{N-f}\right]^e} + \frac{1}{h_w} \right]^{-1} + \frac{\sigma(T_{pm}-T_a)(T_{pm}^2+T_a^2)}{(\varepsilon_p + 0.00591Nh_w)^{-1} + \frac{2N+f+1+0.133\varepsilon_p}{\varepsilon_g} - N} \tag{6}$$

where N is the number of glass cover, ε_g is the glass cover's emissivity, ε_p is the absorber plate's emissivity, σ is the Stefan-Boltzmann constant, and h_w is the heat transfer coefficient of wind.

The edge and back loss coefficients are calculated as:

$$U_e = \frac{k_e}{\delta_e} \times \frac{A_e}{A_c} \tag{7}$$

$$U_b = \frac{k_b}{\delta_b} \tag{8}$$

where A_e signifies edge surface area; k_e and δ_e represent the thermal conductivity and thickness of edge insulation, respectively; k_b and δ_b represent the thermal conductivity and thickness of back insulation, respectively.

The mean temperature (T_{pm}) is computed by assuming an initial value to estimate U_L and Q_u. The next value of T_{pm} is calculated according to the below equation, and the initial value is modified through each iteration [15]:

$$T_{pm} = T_i + \frac{Q_u}{A_p F_R U_L}(1 - F_R) \tag{9}$$

The heat removal factor (F_R) can be expressed as:

$$F_R = \frac{\dot{m}C_p}{A_p U_L}\left[1 - \exp\left(-\frac{F'U_L A_p}{\dot{m}C_p}\right)\right] \tag{10}$$

where C_p is the special heat capacity, and $\dot{m}$ is the mass flow rate.

The collector efficiency factor (F') is:

$$F' = \frac{\frac{1}{U_L}}{W\left(\frac{1}{U_L[D_o + (W-D_o)F]} + \frac{1}{C_b} + \frac{1}{\pi D_i h_{fi}}\right)} \tag{11}$$

where D_o denotes the riser tube's outer diameter, D_i denotes the riser tube's inner diameter, W is the tube spacing, C_b is the thermal conductance of bond, F is the standard fin efficiency, and h_{fi} is the convection heat transfer coefficient.

2.1.2. Economic Analysis

The second objective function for TAC of FPC is determined as [2]:

$$F_2 = C_{total} = aC_{inv} + C_{op} \tag{12}$$

where C_{inv} is investment costs, C_{op} is operational cost, and a is the annual cost factor.

The investment costs of FPC comprise of the capital cost (C_{col}) and pump cost (C_{pump}) as follows [9]:

$$C_{inv} = C_{col} + C_{pump} \tag{13}$$

The operational cost is calculated in equation (14):

$$C_{op} = N_h k_{el} \dot{W}_p \tag{14}$$

where N_h is the system's operational hours per year, and k_{el} is the unit value of electricity.

Annual cost factor (a) is calculated as below:

$$a = \frac{i}{1-(1+i)^{-y}} \tag{15}$$

where y is the lifetime of the system, and i is the inflation rate.

2.2. Problem Formulation for Multiobjective Optimization of FPC

The thermal efficiency and TAC of FPC were considered as two objectives for simultaneous optimization. Hence, the multiobjective optimization of FPC is expressed as follows:

Find: $x^* = [\dot{m}, D_o, N_t, \delta_b]$ (16)

Maximize: $F_1(x^*) = \eta(x^*)$ (17)

Minimize: $F_2(x^*) = C_{total}(x^*)$ (18)

Subject to: $0.01 \le \dot{m} \le 0.1$ (19)

$0.005 \le D_o \le 0.015$ (20)

$6 \le N_t \le 20$ (21)

$0.02 \le \delta_b \le 0.1$ (22)

where the constraints in equations (19) to (22) denote the constraints of the design variables, namely mass flow rate ($\dot{m}$), riser tube's outer diameter (D_o), tube number (N_t), and insulation thickness (δ_b).

If the design variables exceed the restrictions, a repairing approach is applied to adjust the variables as follows:

$$x' = \begin{cases} x_{\max} & \text{if } x > x_{\max} \\ x_{\min} & \text{if } x < x_{\min} \\ x & \text{otherwise} \end{cases} \tag{23}$$

where x signifies the design variable values; x' represents the adjusted design variables values.

3. METHODOLOGY

3.1. Implementation of MOWCA for multiobjective optimization of FPC

The Multiobjective Water Cycle Algorithm (MOWCA) was developed on the basis of observation of the water circulation procedure and the flow process of streams and rivers to the sea. Further details of MOWCA can be found in [16]. To implement the MOWCA to multiobjective optimization of FPC, each individual of the initial population representing the design variables are defined as follows:

$$X_i = [\dot{m}^i, N_t^i, D_o^i, \delta^i]^T \quad \text{for } i = 1,..., N_{pop} \tag{24}$$

The procedures for multiobjective optimization of FPC using MOWCA are stated below:

1. Define the input data, including specifications of FPC and test conditions;
2. Set parameters for the proposed MOWCA: number of population (N_{pop}), summation of number of a sea and rivers (N_{sr}), maximum number of iterations (*Max_Iteration*), evaporation condition constant (d_{max}), and Pareto repository size;
3. The initial population is randomly generated, and initial sea, rivers, and streams are formed via equations as below:

$$Total\ Population = \begin{bmatrix} x_1^1 & x_2^1 & \dots & x_N^1 \\ x_1^2 & x_2^2 & \dots & x_N^2 \\ \vdots & \vdots & \vdots & \vdots \\ x_1^{N_{pop}} & x_2^{N_{pop}} & \dots & x_N^{N_{pop}} \end{bmatrix} \tag{25}$$

$$N_{sr} = Number\ of\ River + 1\ (sea) \tag{26}$$

$$N_{stream} = N_{pop} - N_{sr} \tag{27}$$

4. Fitness function values are calculated for individuals of the initial population:

$$C_i = [F_1(x_1^i, x_2^i, \dots, x_N^i); F_2(x_1^i, x_2^i, \dots, x_N^i)]; \quad \text{for } i = 1, 2, \dots, N_{pop} \tag{28}$$

5. In the initial population, non-dominated solutions are determined and saved in the Pareto repository;

6. Crowding-distance is computed for members in the Pareto repository;

7. A sea and rivers are selected according to the value of crowding-distance;

8. The flow intensity for sea and rivers is determined according to equation (29):

$$NS_n = round\left\{\left|\frac{Cost_n}{\sum_{i=1}^{N_{sr}} Cost_i}\right| \times N_{stream}\right\}; \quad (29)$$

for $n = 1, 2, \ldots, N_{sr}$

9. Streams flow into the rivers via the following correlation:

$$\vec{X}_{Stream}^{i+1} = \vec{X}_{Stream}^{i} + rand \times C \times (\vec{X}_{River}^{i} - \vec{X}_{Stream}^{i}) \quad (30)$$

10. If a stream yields a better solution than the river, the stream's position will exchange with the river's position;

11. Streams can flow into the sea as follows:

$$\vec{X}_{Stream}^{i+1} = \vec{X}_{Stream}^{i} + rand \times C \times (\vec{X}_{Sea}^{i} - \vec{X}_{Stream}^{i}) \quad (31)$$

12. If a stream yields a better solution than the sea, the stream's position will exchange with the sea's position;

13. Rivers flow into the sea by equation (32):

$$\vec{X}_{River}^{i+1} = \vec{X}_{River}^{i} + rand \times C \times (\vec{X}_{Sea}^{i} - \vec{X}_{River}^{i}) \quad (32)$$

14. If a river yields a better solution than the sea, the position of the river will exchange with the sea;

15. Check for evaporation condition;

16. If the evaporation condition is fulfilled, the raining procedure will perform via equation (33):

$$\vec{X}_{Stream}^{new} = L\vec{B} + rand \times (U\vec{B} - L\vec{B}) \quad (33)$$

17. Update d_{max} using equation (34):

$$d_{\max}^{i+1} = d_{\max}^{i} - \frac{d_{\max}^{i}}{Max\_Iteration} \quad (34)$$

18. New non-dominated solutions are determined and saved in the Pareto repository;

19. All dominated solutions are discarded from the Pareto repository;

20. If members in Pareto repository exceed the limit, move to Step 21; if otherwise, move to Step 22;

21. Crowding-distance is computed for members in Pareto repository, and members with the low crowding-distance value are removed;

22. New sea and rivers are selected according to the value of crowding-distance;

23. If the stopping criteria are fulfilled, the optimization process will be ended; if otherwise, back to Step 9.

Figure 2 depicts the MOWCA's flowchart.

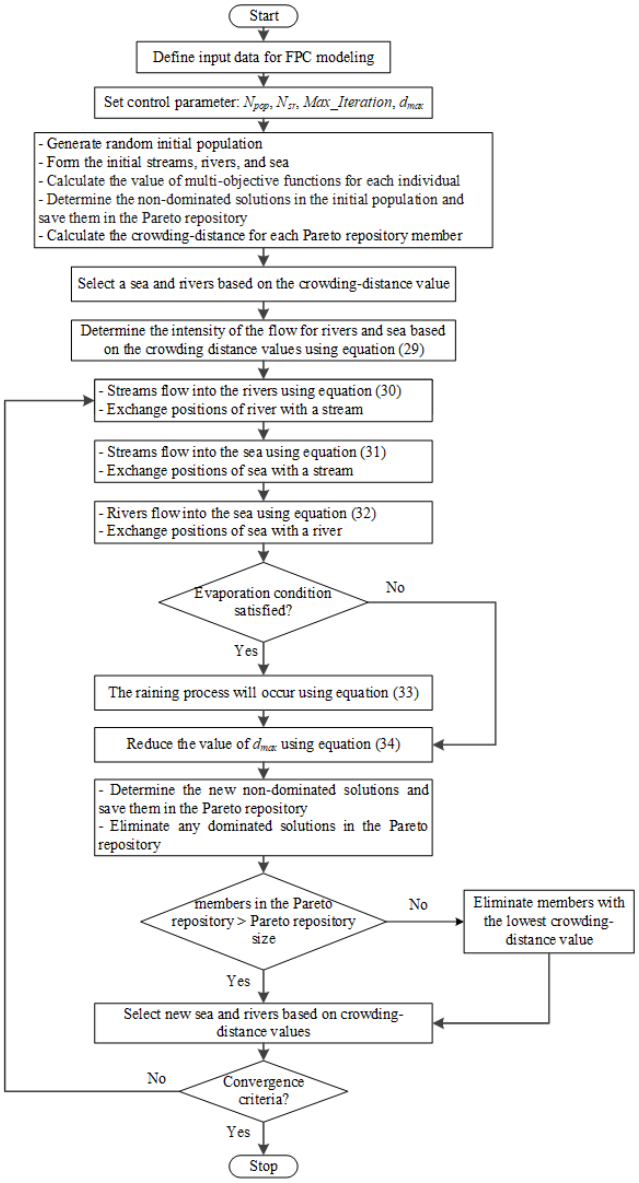

Fig. 2. Flowchart of the MOWCA.

3.2. Decision-making method

The best compromise solution is defined by applying a fuzzy membership function based on Fuzzy Set Theory [17]. First, the linear membership function is given as:

$$\mu_j^k = \begin{cases} 1 & \text{if} \quad f_j^k \le f_j^{\min} \\ \dfrac{f_j^{\max} - f_j^k}{f_j^{\max} - f_j^{\min}} & \text{if} \quad f_j^{\min} \le f_j^k \le f_j^{\max} \\ 0 & \text{if} \quad f_j^k \ge f_j^{\max} \end{cases} \tag{35}$$

where $f_j^{\min}$ and $f_j^{\max}$ are minimum and maximum values of the j^{th} objectives in the non-dominated set, respectively. The normalized membership function μ^k of the k^{th} non-dominated solution can be defined as:

$$\mu^k = \frac{\sum_{j=1}^{n_{obj}} \mu_j^k}{\sum_{k=1}^{n_{pf}} \sum_{j=1}^{n_{obj}} \mu_j^k} \tag{36}$$

where n_{obj} and n_{pf} are numbers of the objective functions and non-dominated solutions, respectively. The solution with a maximally normalized membership function is the best compromise one.

4. NUMERICAL RESULTS

4.1. Optimization results

In this study, the specifications of FPC were referred to the technical details of Kingspan solar collector FPW25 [18]. The unit price for electricity was estimated at 0.10 $/kWh for a system that operated approximately 4,380 h annually. The lifetime of FPC was estimated at 15 years, with an inflation rate of 12%. Table 1 summarizes all characteristics and test conditions of FPC.

Table 1. Specifications and test conditions of FPC

Parameter	Value
Cover surface area (A_c)	2.4213 m^2
Absorber plate area (A_p)	2.2388 m^2
Absorber plate thickness (δ)	0.3 mm
Emissivity of glass cover (ε_g)	0.84
Emissivity of absorber plate (ε_p)	0.04
Effective transmittance-absorptance ($\tau\alpha$)	0.8645
Fluid inlet temperature (T_i)	10°C
Ambient temperature (T_a)	10°C
Total solar radiation intensity (I_T)	1000 W/m^2
Slope of collector (β)	20°
Wind speed (v)	5 m/s

The proposed MOWCA was implemented for multiobjective optimization of the FPC system. The initial parameters of MOWCA (N_{total}, N_{sr}, and d_{max}) were set to 100, 8, and 1E–5, respectively. The number of function evaluations (NFEs) was 10,000, and the number of Pareto optimal solutions was 100.

Figure 3 portrays the Pareto optimal front obtained by MOWCA. These Pareto optimal fronts described the relationship (tradeoff curve) between thermal efficiency and TAC of FPC. These tradeoff curves revealed the confliction between the two selected objectives in the multiobjective optimization situation. An increase in efficiency led to the increasing prevalence of TAC, but the increment slope increased enormously for the highest feasible efficiency.

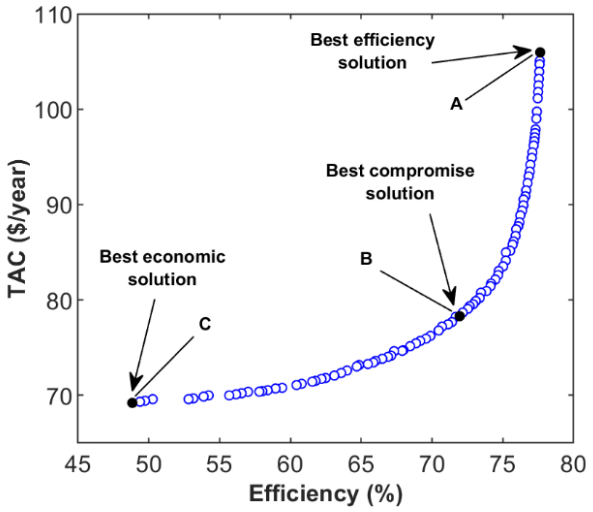

Fig. 3. Pareto optimal front obtained by MOWCA.

Table 2 represents the optimal values of design variables and both objective functions for three solutions A, B, and C. As a critical observation, the maximum values for both thermal efficiency and the TAC were at solution A determined as the best efficiency solution. In contrast, the minimum values for both thermal efficiency and TAC were at solution C defined as the best economic solution. Moreover, the decision-making method was applied to determine the best compromise solution (Solution B). Thus, solution B struck a balance between the two objectives.

Based on obtained solutions in Pareto optimal fronts, decision-makers might select the final solution for a particular project based on specific experiences, desires, and circumstances. If the priority of decision-makers is the performance of FPC, solution A will be the optimal solution. If the priority of decision-makers is given on budget, solution C will be the optimal solution. Additionally, if the manufacturer prefers to achieve a measurable balance between the two objectives, solution C will be the best compromise solution that gives an acceptable efficiency and an affordable cost for FPC.

Table 2. Design parameters and objective function values for Solutions A, B, and C

Parameter	Best efficiency solution (Solution A)	Best compromise solution (Solution B)	Best economic solution (Solution C)
Mass flow rate (m/s)	0.1	0.0646	0.01
Tube diameter (m)	0.015	0.0072	0.005
Tube number	20	19	6
Insulation thickness (m)	0.1	0.0622	0.02
Thermal efficiency (%)	77.6387	71.9541	48.8337
TAC ($/year)	105.9559	78.2980	69.2102

4.2. Statistical comparison and analysis

To assess the proposed method's performance for multiobjective optimization of FPC, MOWCA was run 30 trials independently. Optimization results were compared with three multiobjective methods, including NSGA-II [19], MOPSO [20], and Multiobjective Multi-Verse Optimizer (MOMVO) [21]. For a fair comparison, NFEs was set to 10,000, and the Pareto repository size was kept at 100. Table 3 summarizes control parameters for four algorithms. Obtained results were evaluated based on two performance metrics. Results are illustrated below.

Table 3. Parameters for multiobjective methods

Algorithm	Parameter settings
MOWCA	N_{pop} = 100 N_{sr} = 8 d_{max} = 1E–5
NSGA-II	Population size = 100 Crossover operator = 20 Mutation operator = 20
MOPSO	Population size = 100 Inertia weight = 0.4 Adaptive grid = 30 Mutation rate = 0.5
MOMVO	Population size = 100; Worm hole existence probability max = 1 Worm hole existence probability min = 0.2

4.2.1. Spacing metric

The metric of spacing (*SP*) was proposed by Scott [22] to take into account the distribution of solutions in the Pareto front. This indicator is estimated by measuring a relative distance between successive solutions as follows:

$$SP = \sqrt{\frac{1}{n_{pf}-1}\sum_{i=1}^{n_{pf}}(d_i-\bar{d})^2} \tag{37}$$

$$d_i = \min_j\left(\left|f_1^i(x)-f_1^j(x)\right|-\left|f_2^i(x)-f_2^j(x)\right|\right); \quad \text{for } i, j = 1,2,...,n_{pf} \tag{38}$$

where $\bar{d}$ is the average value of all d_i. An algorithm with a minimum value of *SP* metric has the best uniform distribution in the Pareto front.

Table 4 demonstrates a comparison of four algorithms based on the *SP* metric. Boxplots of the statistical analysis for the *SP* metric yielded by four algorithms are depicted in Figure 4. The distributions of the *SP* metric were illustrated as a rectangle boxplot through which a red line denoted the median for *SP* metric values. The boundary values except the outliers were shown by the top and bottom whiskers in each box plot. The outliers were plotted individually using the '+' symbol.

Table 4. Comparison of multiobjective methods based on SP metric

Algorithm	MOWCA	NSGA-II	MOPSO	MOMVO
Best	0.1768	0.1836	0.2553	0.2776
Mean	0.2109	0.2433	0.6760	0.4818
Worst	0.2431	0.5427	1.0104	0.6820
Std.	0.0144	0.0803	0.2032	0.1205

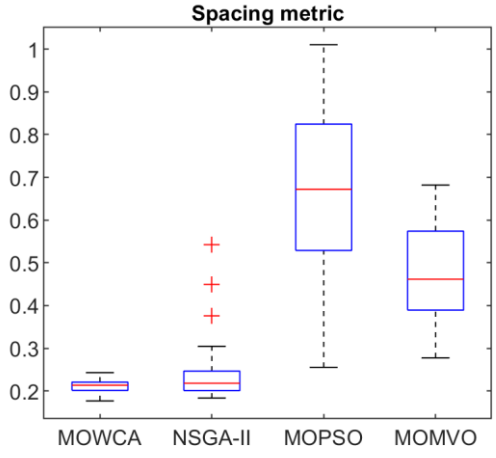

Fig. 4. Box plots of SP metric obtained by different multiobjective methods.

The proposed MOWCA yielded the narrowest boxplot, which was located in the lowest part of the figure. This indicated that the range between the best and the worst value for the *SP* metric was relatively small, as well as least. Moreover, the red line in the boxplot for MOWCA boxplot was lower than other methods, indicating that MOWCA obtained minimal median. It was evident that MOWCA had a robust performance in terms of *SP* metric. From the assessment, the proposed MOWCA found a more evenly distributed Pareto front than other algorithms.

4.2.2. HV metric

The hypervolume (*HV*) indicator is defined as the volume of coverage of the Pareto front in the objective space [23]. This metric evaluates both convergence and diversity of an algorithm. The *HV* metric is computed as follows:

$$HV = \bigcup_{i=1}^{|\Omega|} v_i \tag{39}$$

An algorithm with a high value for the *HV* metric is desirable.

Table 5 summarizes the results of different techniques in terms of the *HV* metric. For comparison, the same reference point was employed for all algorithms in all trials. Figure 5 illustrates the boxplots of the statistical analysis for the *HV* metric yielded by all considered methods. The MOWCA yielded the narrowest boxplot, which was located in the highest part of the figure. Moreover, the red line in the boxplot of MOWCA was higher than other methods. It could be inferred that MOWCA had a robust performance with the highest median value among the four techniques for the *HV* metric. Therefore, MOWCA obtained better convergence and diversity properties of solutions than the other techniques.

Table 5. Comparison of multiobjective methods based on HV metric

Algorithm	MOWCA	NSGA-II	MOPSO	MOMVO
Best	1498.3096	1494.2236	1470.6501	1488.2148
Mean	1497.6856	1490.1943	1458.2522	1483.5239
Worst	1496.4985	1483.4197	1441.4022	1476.9831
Std.	0.4209	2.6880	7.6663	3.0906

Although the FPC modeling was effectively optimized in the case mentioned above study, some limitations should be addressed to improve the FPC optimization model. The MOWCA should be implemented with large scale FPC systems. This study also showed the potential of the proposed MOWCA in multiobjective optimization of FPC. However, MOWCA should be modified and improved to achieve better solution quality and faster computation time.

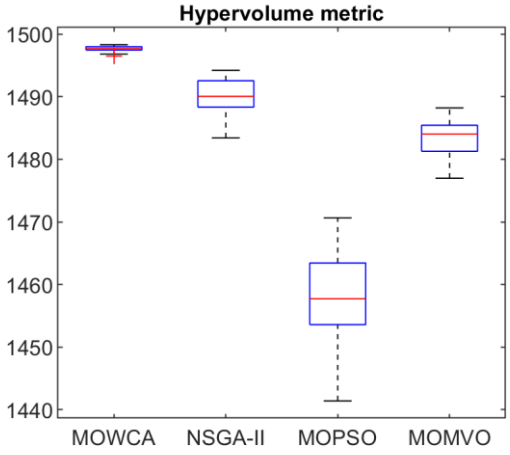

Fig. 5. Box plots of HV metric obtained by different multiobjective methods.

5. CONCLUSION

This paper suggested MOWCA for multiobjective optimization of FPC, in which the thermal efficiency and TAC of FPC were optimized simultaneously. The obtained results were analyzed and compared with other optimization techniques using SP and HV metrics. The proposed MOWCA provided a superior quality of solutions in comparison with the other well-known algorithms. The Pareto optimal front generated by the MOWCA was considered to be a beneficial approach, assisting manufacturers in determining the optimal tradeoff among the two important considerations of the thermal efficiency and TAC for FPC. For further research, MOWCA should be implemented for multiobjective optimization in other solar thermal systems such as concentrated solar power and solar power tower.

ACKNOWLEDGMENTS

We acknowledge the support of time and facilities from Ho Chi Minh City University of Technology (HCMUT), VNU-HCM for this study.

ABBREVIATION

FPC	flat plate collector
HV	hypervolume indicator
MOMVO	Multiobjective Multi-Verse Optimizer
MOPSO	Multiobjective Particle Swarm Optimization
MOWCA	Multiobjective Water Cycle Algorithm
NSGA-II	Nondominated Sorting Genetic Algorithm II
SP	metric of spacing
SWH	solar water heating system
TAC	total annual cost

NONMENCLATURE

a	annual cost factor
A_c	cover surface area
A_e	edge surface area
A_p	absorber plate area
C_b	thermal conductance of the bond
C_p	specific heat capacity
C_{col}	collector capital cost
C_{inv}	investment costs
C_{op}	operational cost
C_{pump}	pump cost
C_{total}	total annual cost
D_i	riser tube's inner diameter
D_o	riser tube's outer diameter
d_{max}	evaporation condition constant
F	standard fin efficiency
F'	collector efficiency coefficient
F_R	heat removal coefficient
h_{fi}	convection heat transfer coefficient
h_w	heat transfer coefficient of the wind
i	inflation rate
I_T	total solar radiation intensity
k_b	back insulation's thermal conductivity
k_e	edge insulation's thermal conductivity
k_{el}	unit value of electricity
$Max\_Iteration$	maximum number of iterations
N	number of covers
N_h	system's operational hours per year
N_{pop}	population size
N_{sr}	summation of number of a sea and rivers
N_t	tube number
Q_{ab}	absorbed energy
Q_{loss}	total heat loss
Q_u	useful heat gain
T_a	ambient temperature
T_i	inlet temperature
T_{pm}	absorber plate's mean temperature
U_b	back loss coefficient
U_e	edge loss coefficient
U_L	overall heat loss coefficient
U_t	top loss coefficient
W	tube spacing
y	lifetime of the system
β	slope of the collector
δ_b, δ_e	thickness of back insulation and edge insulation, respectively
ε_g, ε_p	emissivity of the glass cover and absorber plate, respectively
$\dot{m}$	fluid mass flow rate
η	thermal efficiency of FPC system
σ	Stefan-Boltzmann constant
$(\tau\alpha)$	effective transmittance-absorptance

REFERENCES

[1] O. L. Jing, M. J. K. Bashir, and J.-J. Kao, "Solar radiation based benefit and cost evaluation for solar water heater expansion in Malaysia," *Renewable and Sustainable Energy Reviews*, vol. 48, pp. 328–335, Aug. 2015, doi: 10.1016/j.rser.2015.04.031.

[2] Z. Hajabdollahi and H. Hajabdollahi, "Thermo-economic modeling and multi-objective optimization of solar water heater using flat plate collectors," *Solar Energy*, vol. 155, pp. 191–202, Oct. 2017, doi: 10.1016/j.solener.2017.06.023.

[3] T. H. Huy, P. Nallagownden, and R. Kannan, "Energetic Optimization of Solar Water Heating System with Flat Plate Collector using Search Group Algorithm," vol. 61, no. 2, p. 17, 2019.

[4] S. Farahat, F. Sarhaddi, and H. Ajam, "Exergetic optimization of flat plate solar collectors," *Renewable Energy*, vol. 34, no. 4, pp. 1169–1174, Apr. 2009, doi: 10.1016/j.renene.2008.06.014.

[5] F. Jafarkazemi and E. Ahmadifard, "Energetic and exergetic evaluation of flat plate solar collectors," *Renewable Energy*, vol. 56, pp. 55–63, Aug. 2013, doi: 10.1016/j.renene.2012.10.031.

[6] O. Badr, A. Mohammed, and D. Brahim, "Optimization of the Thermal Performance of the Solar Water Heater (SWH) Using Stochastic Technique," p. 10, 2018.

[7] K. Y. Wenceslas and T. Ghislain, "Experimental Validation of Exergy Optimization of a Flat-Plate Solar Collector in a Thermosyphon Solar Water Heater," *Arab J Sci Eng*, vol. 44, no. 3, pp. 2535–2549, Mar. 2019, doi: 10.1007/s13369-018-3227-x.

[8] M. Khademi, F. Jafarkazemi, E. Ahmadifard, and S. Younesnejad, "Optimizing Exergy Efficiency of Flat Plate Solar Collectors Using SQP and Genetic Algorithm," *AMM*, vol. 253–255, pp. 760–765, Dec. 2012, doi: 10.4028/www.scientific.net/AMM.253-255.760.

[9] F. Hajabdollahi and K. Premnath, "Numerical study of the effect of nanoparticles on thermoeconomic improvement of a solar flat plate collector," *Applied Thermal Engineering*, vol. 127, pp. 390–401, Dec. 2017, doi: 10.1016/j.applthermaleng.2017.08.058.

[10] H. Hajabdollahi, "Investigating the effect of nanofluid on optimal design of solar flat plate collector," in *2018 5th International Conference on Renewable Energy: Generation and Applications (ICREGA)*, Feb. 2018, pp. 188–191, doi: 10.1109/ICREGA.2018.8337594.

[11] Z. Hajabdollahi, H. Hajabdollahi, and K. C. Kim, "Multi-objective optimization of solar collector using water-based nanofluids with different types of nanoparticles," *J Therm Anal Calorim*, Jun. 2019, doi: 10.1007/s10973-019-08444-w.

[12] S. A. Kalogirou, "Solar thermal collectors and applications," *Progress in Energy and Combustion Science*, vol. 30, no. 3, pp. 231–295, Jan. 2004, doi: 10.1016/j.pecs.2004.02.001.

[13] J. A. Duffie and W. A. Beckman, "Solar Engineering of Thermal Processes," p. 928.

[14] V. K. Agarwal and D. C. Larson, "Calculation of the top loss coefficient of a flat-plate collector," *Solar Energy*, vol. 27, no. 1, pp. 69–71, Jan. 1981, doi: 10.1016/0038-092X(81)90022-0.

[15] O. Mahian, A. Kianifar, A. Z. Sahin, and S. Wongwises, "Heat Transfer, Pressure Drop, and Entropy Generation in a Solar Collector Using SiO2/Water Nanofluids: Effects of Nanoparticle Size and pH," *J. Heat Transfer*, vol. 137, no. 6, pp. 061011-061011–9, Jun. 2015, doi: 10.1115/1.4029870.

[16] A. Sadollah, H. Eskandar, and J. H. Kim, "Water cycle algorithm for solving constrained multi-objective optimization problems," *Applied Soft Computing*, vol. 27, pp. 279–298, Feb. 2015, doi: 10.1016/j.asoc.2014.10.042.

[17] W. Sheng, K.-Y. Liu, Y. Liu, X. Meng, and Y. Li, "Optimal Placement and Sizing of Distributed Generation via an Improved Nondominated Sorting Genetic Algorithm II," *IEEE Transactions on Power Delivery*, vol. 30, no. 2, pp. 569–578, Apr. 2015, doi: 10.1109/TPWRD.2014.2325938.

[18] "Flat Plate Panels," *Kingspan | USA*. https://www.kingspan.com/us/en-us/product-groups/renewable-technologies/solar-thermal/solar-flat-plate-panels/flat-plate-panels (accessed Nov. 06, 2019).

[19] K. Deb, A. Pratap, S. Agarwal, and T. Meyarivan, "A fast and elitist multiobjective genetic algorithm: NSGA-II," *IEEE Transactions on Evolutionary Computation*, vol. 6, no. 2, pp. 182–197, Apr. 2002, doi: 10.1109/4235.996017.

[20] C. A. C. Coello, G. T. Pulido, and M. S. Lechuga, "Handling multiple objectives with particle swarm optimization," *IEEE Transactions on Evolutionary Computation*, vol. 8, no. 3, pp. 256–279, Jun. 2004, doi: 10.1109/TEVC.2004.826067.

[21] S. Mirjalili, P. Jangir, S. Z. Mirjalili, S. Saremi, and I. N. Trivedi, "Optimization of problems with multiple objectives using the multi-verse optimization algorithm," *Knowledge-Based Systems*, vol. 134, pp. 50–71, Oct. 2017, doi: 10.1016/j.knosys.2017.07.018.

[22] J. R. (Jason R. Schott, "Fault tolerant design using single and multicriteria genetic algorithm optimization," Thesis, Massachusetts Institute of Technology, 1995.

[23] K. Deb and D. Kalyanmoy, *Multi-Objective Optimization Using Evolutionary Algorithms*. USA: John Wiley & Sons, Inc., 2001.